

# Sodium-Directed Photon-Induced Assembly Strategy for Preparing Multisite Catalysts with High Atomic Utilization Efficiency

Xiaoqiang An, Tingcha Wei, Peijia Ding, Li-Min Liu, Lunqiao Xiong, Junwang Tang, Jiani Ma, Feng Wang, Huijuan Liu and Jiuhui Qu

The self-archived postprint version of this journal article is available at Linköping University Institutional Repository (DiVA):

<https://urn.kb.se/resolve?urn=urn:nbn:se:liu:diva-196935>

N.B.: When citing this work, cite the original publication.

An, X., Wei, T., Ding, P., Liu, L., Xiong, L., Tang, J., Ma, J., Wang, F., Liu, H., Qu, J., (2023), Sodium-Directed Photon-Induced Assembly Strategy for Preparing Multisite Catalysts with High Atomic Utilization Efficiency, *Journal of the American Chemical Society*, 145(3), 1759-1768.  
<https://doi.org/10.1021/jacs.2c10690>

Original publication available at:

<https://doi.org/10.1021/jacs.2c10690>

Copyright: American Chemical Society

<https://pubs.acs.org/>

# A sodium-mediated photoreconstruction strategy to regulate metal dispersion on TiO<sub>2</sub> for multi-site synergistic catalysis

Xiaoqiang An<sup>a</sup>, Tingcha Wei<sup>a,b</sup>, Li-Min Liu<sup>c</sup>, Lunqiao Xiong<sup>d</sup>, Junwang Tang<sup>d</sup>,  
Huijuan Liu<sup>a</sup>, Jiuhui Qu<sup>a</sup>

<sup>a</sup> Center for Water and Ecology, State Key Joint Laboratory of Environment Simulation and Pollution Control, School of Environment, Tsinghua University, Beijing 100084

<sup>b</sup> China College of Science, Nanjing University of Aeronautics and Astronautics, Nanjing 211106, China

<sup>c</sup> School of Physics, Beihang University, Beijing 100191, China

<sup>d</sup> Department of Chemical Engineering, University College London, Torrington Place, London WC1E 7JE, UK

Department of Physics, Chemistry and Biology (IFM), Linköping University, Linköping 581 83, Sweden

**Abstract:** Combined atomic sites can offer new prospects to address the current difficulties in single-atom catalysis, but accurately constructing multifarious sites and rationally regulating their synergistic interactions have remained challenging. Here, we report a sodium-mediated photoreconstruction strategy to synthesize multi-site photocatalysts through interfacial redispersion of noble metal atoms over support materials for enhanced catalysis. Residual Na<sup>+</sup> on TiO<sub>2</sub> surface was employed to stabilize Au single atoms and mediate the unique Au-TiO<sub>2</sub> interactions. A light-induced reconstruction procedure was performed to reassemble neighboring Au atoms into nanocluster via a solid–solid route. Advanced characterizations revealed that the charge transfer between light-excited supports and Au(Na<sup>+</sup>) ensembles enabled the redispersion of Au atoms on TiO<sub>2</sub> for the bottom-up construction of plasmonic fields. In the resulting photocatalyst, the cascade electron transfer from assembled Au nanoclusters to defective TiO<sub>2</sub> nanosheets and sodium-stabilized Au single atoms contributed to a nearly two orders of magnitude improvement in plasmon-enhanced hydrogen evolution over TiO<sub>2</sub> under simulated solar light, with a record TON<sub>Au</sub> value

of 4600. Our reconstruction strategy proved effective in atomic-scale regulation of various noble metal-cocatalyzed protocols for synergistic catalysis. This study provides a well-defined platform to extend the boundaries of SACs for multi-site synergistic catalysis through harnessing metal-support interactions.

**KEYWORDS:** Bottom-up assembly, photoreconstruction, single atoms, photocatalytic water splitting, metal-support interactions

## Introduction

Single-atom catalysts (SACs) have attracted considerable attention in recent years, due to the maximum utilization efficiency of metal atoms, especially for noble metals that usually act as highly reactive sites for photocatalytic reactions.<sup>[1,2]</sup> Although much progress has been made in the past few years, single atoms with high surface energy are susceptible to agglomeration, posing a significant challenge of catalyst stability for further development.<sup>[3]</sup> In addition, the performance of SACs is far from the theoretical maximum efficiency of atomic utilization, as the simplicity of single-atom sites makes it difficult to break linear scaling relationships between adsorption energies of reaction intermediates.<sup>[4]</sup> Recent studies suggest that the above issues can be addressed by creating combined atomic sites in SACs, such as dual-metal dimers, single-atom alloys, and nanoclusters.<sup>[5-7]</sup> In these protocols, coupling different sites could induce the redistribution of metal charges and optimize the adsorption/desorption of intermediates, thereby effectively improving the catalytic performance.<sup>[8,9]</sup> However, a significant challenge in developing this kind of catalyst is the difficulty of precisely controlling the formation of multifarious sites and their interactions under synthesis conditions.<sup>[10]</sup>

Supported SACs with the inherent structure complexities of the underlying substrates, such as terminal groups, defects, and surface impurities, play a decisive role in tuning the coordination environment and stability of metal active sites.<sup>[11]</sup> From a synthesis perspective, the spatial distribution of dispersed metal atoms on a support material could be regulated by the metal-support interplay. This enables the possibility of redispersing supported single atoms via solid-state reactions, which can not only give rise to a bottom-up approach to construct multifarious atomically dispersed sites but also offer an opportunity to overcome the challenge of stability in SACs.<sup>[12]</sup>

Nevertheless, how one can manipulate the metal–support interactions in SACs remains an open question, and the application of this principle in site engineering of SACs has not been intentionally attempted yet.<sup>[13]</sup>

Here, we demonstrate a sodium-mediated photoreconstruction (denoted as SPR) strategy to construct multifarious atomic sites on 001-faceted TiO<sub>2</sub> nanosheets for synergistic photocatalysis (Figure 1a). This SPR strategy includes two steps: i) the formation of Au single atoms on TiO<sub>2</sub> with the assistance of Na<sup>+</sup> as an adherent mediator to regulate the Au–TiO<sub>2</sub> interactions,<sup>[14]</sup> and ii) the formation of Au nanoclusters from self-assembling partial Au single atoms under light illumination. As demonstrated by advanced characterization techniques and theoretical simulations, sodium could stabilize the proximal Au single atoms on the TiO<sub>2</sub> surface by decreasing the length of the Au–O bond (Figure S1). Light radiation of presynthesized catalyst powders triggered the transfer of photogenerated electrons from Ti<sup>3+</sup> to Au(Na<sup>+</sup>) ensembles, thereby bottom-up assembled neighboring Au single atoms into Au nanoclusters with surface plasmon resonance.<sup>[15]</sup> To further promote the charge transfer, we performed vacuum heating to create oxygen vacancy (O<sub>v</sub>) defects in TiO<sub>2</sub> as an electron shuttler. As such, the synthesized Au nanoclusters/TiO<sub>2</sub> with oxygen vacancies/Au single atoms (SC-Au/O<sub>v</sub>-TiO<sub>2</sub>) photocatalyst exhibited an unprecedented hydrogen evolution rate of 4.37 mmol g<sup>−1</sup> h<sup>−1</sup> with the TON<sub>Au</sub> value of 4600, representing a new record amongst Au catalyzed TiO<sub>2</sub> photocatalysts. Moreover, our SPR strategy was proved to be universal for refining the active sites of various SASSs, including atomically dispersed Pt, Pd, Au, and their alloys on TiO<sub>2</sub>, BiOBr, and CeO<sub>2</sub> for versatile applications.

## Results and Discussion

**Photocatalytic properties of site-engineered TiO<sub>2</sub> nanosheets.** 001-faceted TiO<sub>2</sub> nanosheets were synthesized by a typical hydrothermal method (Figure 1b, Figure S2 and S3), followed by NaOH solution washing with the formation of sodium modified TiO<sub>2</sub> nanosheets (detailed procedures in SI). The uniform distribution of Au single atoms on wet-impregnated TiO<sub>2</sub> (S-Au/TiO<sub>2</sub>) could be identified by the numerous bright contrast spots (Figure 1c) on nanosheets in transmission electron microscopy (TEM) and high-angle annular dark-field scanning transmission electron microscopy

(HAADF-STEM). For photoreconstructed sample (SC-Au/TiO<sub>2</sub>), Au nanoclusters with an average diameter of 1.4 nm (ca. 90 atoms per cluster, Figure 1d) were observed together with some isolated Au single atoms, suggesting the successful construction of synergistic atomic sites on TiO<sub>2</sub> supports.

Photocatalytic hydrogen evolution reactions were performed to evaluate the activities of atomic-level engineered photocatalysts. Under simulated solar light irradiation, pristine TiO<sub>2</sub> presented poor activity for water splitting, with a hydrogen evolution rate of 0.05 mmol g<sup>-1</sup> h<sup>-1</sup> (Figure 1e). The introduction of Au single atoms as cocatalysts enhanced the activity by 30 times, with a H<sub>2</sub> evolution rate of 1.5 mmol h<sup>-1</sup> g<sup>-1</sup>, which was 2 times higher than the benchmark sample synthesized by the traditional photodeposition method (P-Au/TiO<sub>2</sub>) (Figure S4). SC-Au/TiO<sub>2</sub> with multifarious metal sites exhibited an additional 2-fold increase in photoactivity. With the creation of oxygen vacancies (O<sub>v</sub>) in TiO<sub>2</sub> by vacuum heating (Figure S5), the final SC-Au/O<sub>v</sub>-TiO<sub>2</sub> showed an unprecedented hydrogen evolution rate of 4.37 mmol g<sup>-1</sup> h<sup>-1</sup>, which was nearly two orders of magnitude higher than pristine 001-TiO<sub>2</sub>.<sup>[16]</sup> When normalized by the weight of Au content, the TON<sub>Au</sub> value was 4600 after three hours under simulated solar light, which represented a new record of atom utilization efficiency for Au cocatalyzed TiO<sub>2</sub> (Figure 1f and Table S1).<sup>[17-26]</sup> In addition, the photocatalysts exhibited good reproducibility of H<sub>2</sub> evolution without any obvious decrease after an 18 h test (Figure 1g). This was also verified by the retained single-atom sites and Au clusters in recycled catalysts (Figure S6). Moreover, the SPR strategy was applicable to construct a series of TiO<sub>2</sub>-based nanoarchitectures with multifarious cocatalyst sites, such as Pt- and Pd-cocatalyzed 001-TiO<sub>2</sub>, dual metal cocatalyzed 001-TiO<sub>2</sub> and Au cocatalyzed 101-TiO<sub>2</sub> (Figure 1h, Figure S7). All reconstructed samples exhibited more than two times higher catalytic activity than the corresponding single-atom photocatalysts (Figure S8), confirming the benefit of synergistic sites for high-performance catalysts.

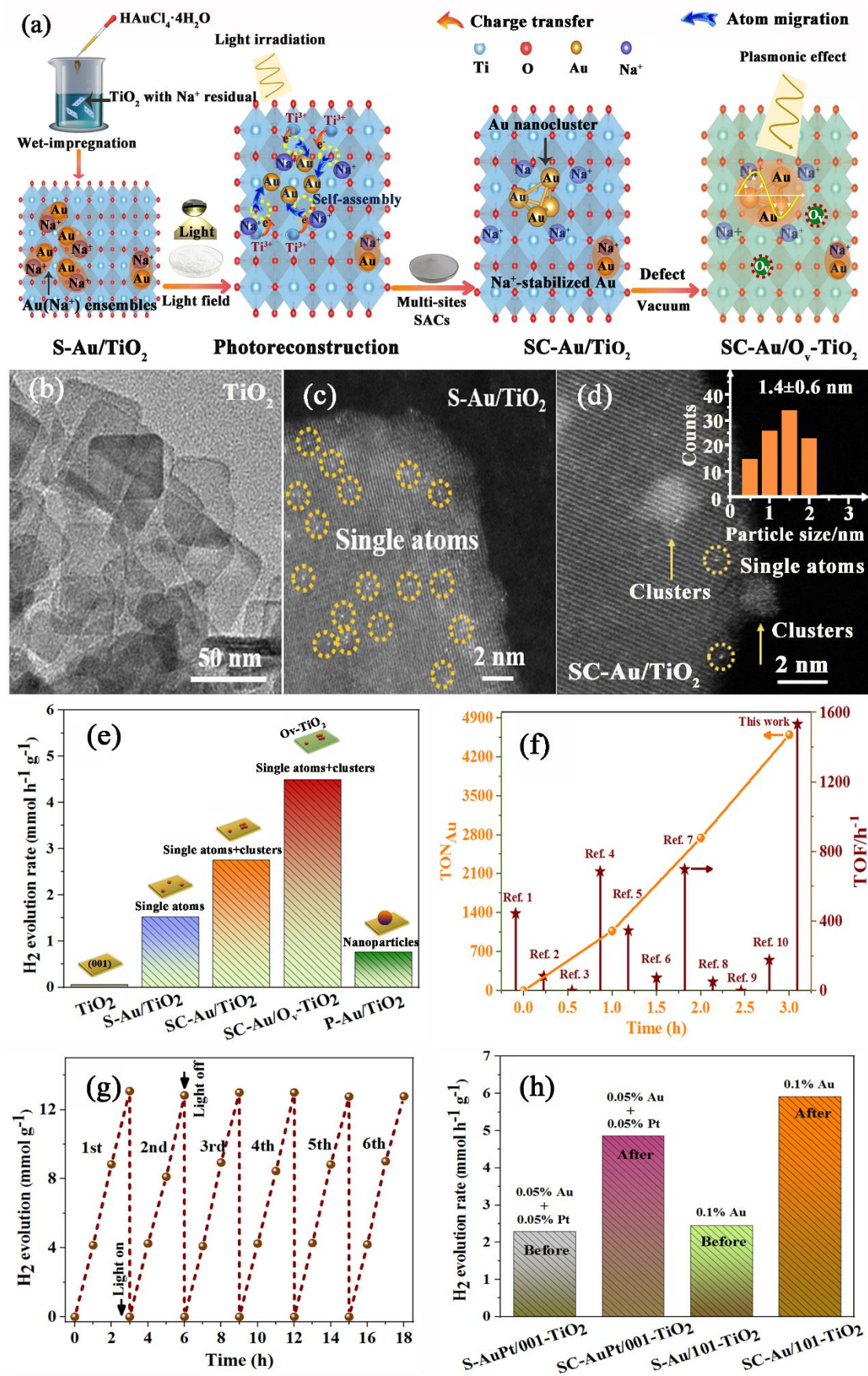


**Figure 1** (a) Schematic illustration of the Na-mediated photoreconstruction strategy; (b)

TEM image of TiO<sub>2</sub>; (c, d,) HAADF-STEM images of S-Au/TiO<sub>2</sub> (c) and SC-Au/TiO<sub>2</sub> (d). Inset of (d) is the size distribution curve of Au clusters in SC-Au/TiO<sub>2</sub>; (e) Time-dependent H<sub>2</sub> evolution over TiO<sub>2</sub> cocatalyzed by different types of metal sites under simulated solar light irradiation (AM1.5G); (f) Calculated TON<sub>Au</sub> after 3 h simulated sunlight irradiation and comparing photoactivity of photoreconstructed SC-Au/O<sub>v</sub>-TiO<sub>2</sub> with reported results; (g) Cycling measurements of photocatalytic hydrogen production over SC-Au/O<sub>v</sub>-TiO<sub>2</sub> for 18 hours; (h) Photoreconstruction of diverse atomically dispersed cocatalysts on TiO<sub>2</sub> for performance improvement.

**Roles of sodium and light illumination for site reconstruction.** The first critical part of our strategy was the residual sodium on TiO<sub>2</sub> nanosheets (originated from NaOH used for removing fluorine, Figure S9) that acted as an adherent mediator to promote the formation of Au single atoms. This could be indicated by the fact that less amount of Au atoms were anchored onto TiO<sub>2</sub> without the assistance of sodium (Figure S10), with a sharply decreased H<sub>2</sub> evolution capability of the corresponding reconstructed sample (Figure S11). To understand the detailed function of Na<sup>+</sup>, we firstly perform inductively coupled plasma optical emission spectrometry (ICP-OES) measurements to estimate the amount of Na<sup>+</sup>. The results indicated the weight contents of Au and Na<sup>+</sup> in all Au-loaded samples are almost equivalent (0.07 wt% of TiO<sub>2</sub>) (Table S2). Considering it is difficult to visualize the Na<sup>+</sup>, its electronic structure before and after Au atoms formation was investigated by X-ray photoelectron spectroscopy (XPS). As shown in Figure 2a, the binding energy of Na 1s at ~1072 eV in TiO<sub>2</sub> samples corresponded to the ionic state of Na<sup>+</sup> residual. Interestingly, this peak shifted to lower bind energy after the introduction of Au single atoms, implying the strong coupling effect between Au and Na<sup>+</sup>.<sup>[27]</sup> This can also be verified by X-ray absorption near-edge structure (XANES) and nuclear magnetic resonance (NMR) spectroscopy. As expected, we observed the decreased oxidation density of Na<sup>+</sup> in S-Au/TiO<sub>2</sub> based on the decreased intensity of the white line peak in the normalized XANES spectra (Figure 2b).<sup>[28]</sup> In the NMR spectra, the shift of the <sup>23</sup>Na signal toward a high field further confirmed the increased electron density of Na<sup>+</sup> (Figure 2c). Density functional theory (DFT) calculations were performed to deeply understand the mediation effect of sodium

during site reconstruction. We found that a single Au atom was prone to be linked to surface  $O_{2c}$  of 001- $TiO_2$  by Au-O bond. The modification of  $TiO_2$  by  $Na^+$  decreased the length of Au-O bond from 3.26 Å of pure  $TiO_2$  to 2.17 Å (Figure S12). It signified that atomically dispersed Au could be firmly anchored on the surface of  $Na^+$ -modified  $TiO_2$  via the oxygen linkages (Figure S13),<sup>[29]</sup> forming evolutionary ensembles similar to  $Au-O(OH)_x$  in the reported alkali-promoted water-gas-shift catalysts.<sup>[30]</sup>

The second critical part of our strategy was the reconstruction of partial Au single atoms into nanoclusters with the assistance of light illumination. We systematically investigated the transformation details by XPS, XANES, and extended X-ray absorption fine structure (EXAFS). In contrast to the metallic Au ( $Au^0$ ) in benchmark P-Au/ $TiO_2$ , Au single atoms presented +1 oxidation state ( $Au^+$ ) in S-Au / $TiO_2$ , as evidenced by the shift of Au 4f<sub>7/2</sub> and Au 4f<sub>5/2</sub> peaks toward lower binding energies in the XPS spectra (Figure 2d). Light irradiation of presynthesized S-Au / $TiO_2$  powders led to the appearance of metallic Au species ( $Au^0$ ), corresponding to the formation of Au nanoclusters. The decreased oxidation state of Au nanoclusters in SC-Au/ $TiO_2$  could be observed in XANES and EXAFS, as the white line intensity was between the intensities of S-Au/ $TiO_2$  and Au foil (Figure 2e).<sup>[31]</sup> We further conducted Wavelet transform (WT) and compared the Fourier transforms (FT) curves of Au L<sub>3</sub>-edge in EXAFS to analyze the coordination environment of Au in different samples. In S-Au/ $TiO_2$ , the WT maximum correlated with Au-O bonds located at 1.6 Å (Figure 2f), which was in good agreement with the theoretically calculated value (The R-space value should be corrected by ~0.4 Å, due to the  $k$  dependence of total phase shift),<sup>[32]</sup> confirming the stabilization of Au single atoms on the sodium modified  $TiO_2$ . While in SC-Au/ $TiO_2$ , the appearance of an additional Au-Au bond at 2.5 Å confirmed the partial conversion of Au single atoms into metallic nanoclusters. Combined with the Au 4f deconvolution results, the percentages of  $Au^+$  and  $Au^0$  were calculated to be around 63% and 37%, respectively. Another interesting result is the change of the chemical environment of  $Na^+$  after light illumination. As mentioned in the last paragraph (Figure 2a), the electron density of  $Na^+$  on  $TiO_2$  increased after the introduction of Au single atoms. While the formation of nanocluster restored the electron density of  $Na^+$  close to



that of in pristine  $\text{Na}^+$  modified  $\text{TiO}_2$ , implying the separation of partial  $\text{Au}(\text{Na}^+)$  ensembles during photoreconstruction.

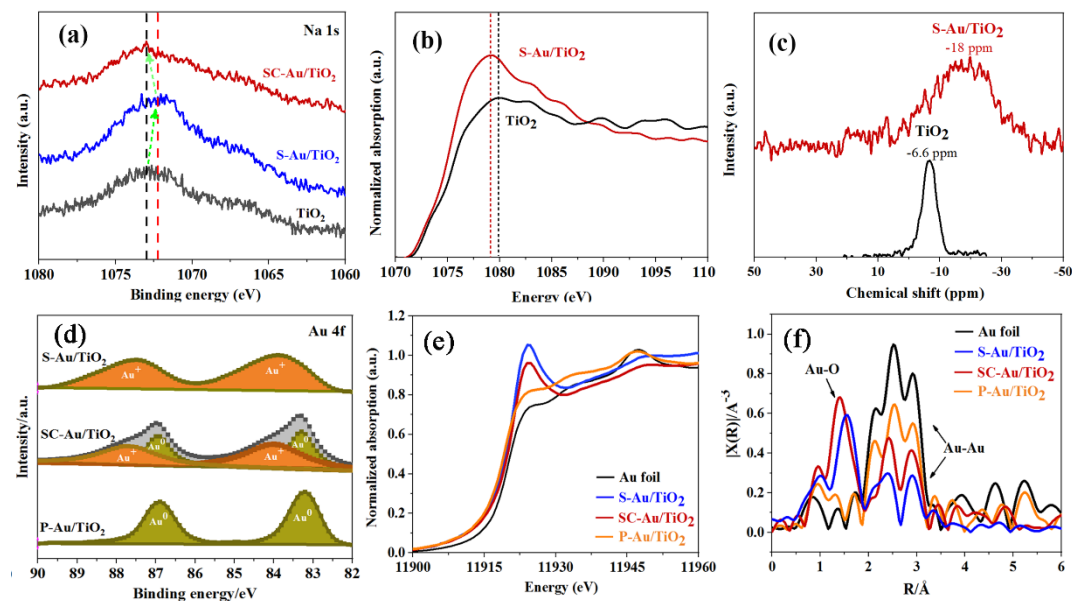


**Figure 2** (a) Na 1s XPS spectra of  $\text{TiO}_2$ , S-Au/ $\text{TiO}_2$ , and SC-Au-TiO<sub>2</sub>; (b) Na K-edge XANES spectra of  $\text{TiO}_2$  and S-Au/ $\text{TiO}_2$ ; (c)  $^{23}\text{Na}$  NMR spectra of  $\text{TiO}_2$  and S-Au/ $\text{TiO}_2$ ; (d) Au 4f XPS spectra, (e) Au L<sub>3</sub>-edge XANES spectra of different photocatalysts. (f) Fourier transform (FT) Au L<sub>3</sub>-edge (k) of different photocatalysts.

To understand the underlying mechanism of Na-mediated photoreconstruction, we firstly studied the interplay between Au and  $\text{TiO}_2$  by XPS analysis (Figure S14). As shown in Figure 3a, the binding energy of Ti 2p was decreased after the introduction of Au single atoms, indicating a strong interaction between  $\text{Au}(\text{Na}^+)$  ensembles and  $\text{TiO}_2$  supports, consistent with the formation of Au-O bond as mentioned above. We employed synchronous XPS to in-situ monitor the chemical environment of Ti in pristine  $\text{TiO}_2$  and S-Au-TiO<sub>2</sub> upon light illumination. As shown in Figure 3b, the illumination shifted the Ti 2p peak to a lower value, which could be explained by the generation of delocalized electrons. Interestingly, the binding energy of Ti 2p in S-Au/ $\text{TiO}_2$  showed an opposite shift upon illumination, implying the restructuring of cocatalyst sites via the electron transfer from excited  $\text{TiO}_2$  to Au single atoms. This process could also be assessed by the quasi-in-situ electron spin resonance (ESR) experiments. As shown in Figure 3c, pristine  $\text{TiO}_2$  exhibited an intense resonance signal at  $g=2.004$  under illumination, attributed to the trapping of photogenerated electrons by

oxygen vacancies. However, this signal disappeared in S-Au/TiO<sub>2</sub> and a sharp spin peak from Ti<sup>3+</sup> at g=1.98 emerged.<sup>[33]</sup> Under continuous illumination, the Ti<sup>3+</sup> signal weakened and shifted to g=1.977, confirming the electron transfer from excited TiO<sub>2</sub> to sodium-stabilized Au single atoms via Ti<sup>3+</sup>. With reducing capability, these transferred electrons could practically weaken the Au-O bond, thereby facilitating the agglomeration of adjacent Au single atoms into nanoclusters.<sup>[34]</sup>

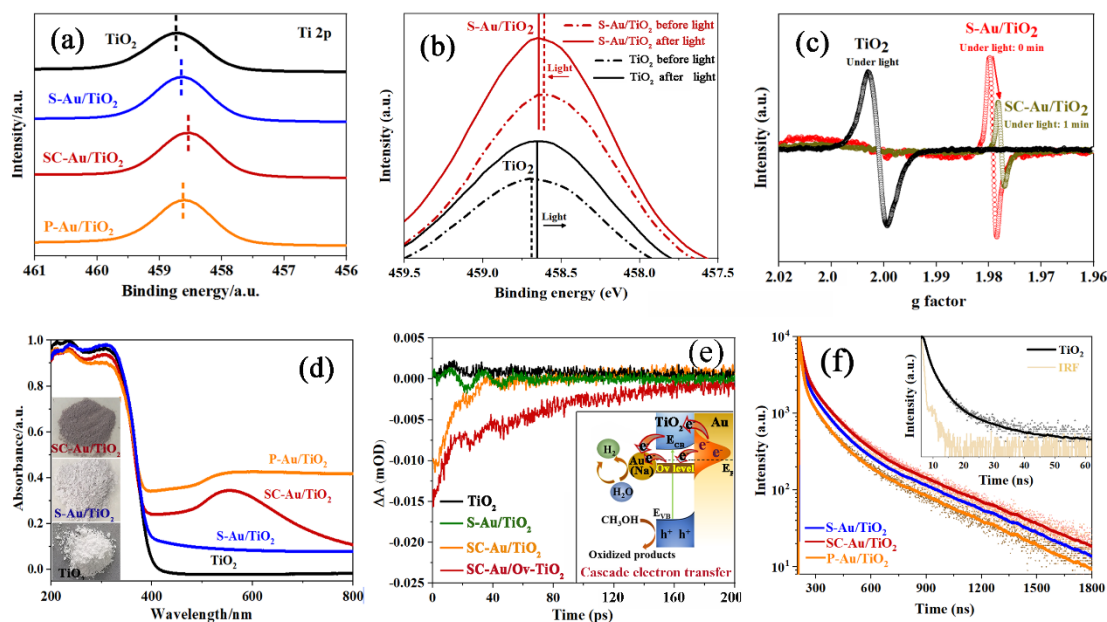


**Figure 3** (a) Ti 2p XPS spectra of different photocatalysts; (b) Synchronous illumination XPS spectra of TiO<sub>2</sub> and S-Au/TiO<sub>2</sub>; (c) ESR spectra of TiO<sub>2</sub> and S-Au/TiO<sub>2</sub> under light irradiation; (d) UV-vis DRS of different samples. Insets show the photographs of TiO<sub>2</sub>, S-Au/TiO<sub>2</sub>, and SC-Au/TiO<sub>2</sub>; (e) Transient absorption kinetics probed at 550 nm for TiO<sub>2</sub>, S-Au/TiO<sub>2</sub>, SC-Au/TiO<sub>2</sub>, and SC-Au/O<sub>v</sub>-TiO<sub>2</sub>. Inset shows the synergistic mechanism of SC-Au/O<sub>v</sub>-TiO<sub>2</sub> for plasmonic water splitting; (f) Time-resolved photoluminescence (TRPL) decay curves of different samples. Inset displays the curve of blank TiO<sub>2</sub> and the instrument response function (IRF).

**Mechanism of multi-site synergistic catalysis.** We now turn to reveal the working mechanism of synergistic sites in SC-Au/O<sub>v</sub>-TiO<sub>2</sub> for activity enhancement. UV-vis diffuse reflectance spectroscopy (UV-vis DRS) showed that the absorption edge of pristine TiO<sub>2</sub> was located around 400 nm, and the introduction of Au single atoms slightly impact the absorption property of TiO<sub>2</sub> (Figure 3d). After the reconstruction of

Au atoms, SC-Au/TiO<sub>2</sub> exhibited a broad plasmonic absorption centered at 550 nm with a color of dark purple (Inset of Figure 3d), indicating the creation of an oscillating electromagnetic field by the bottom-up assembly of Au sites. The kinetics of hot carrier transfer was thereafter evaluated by TAS using a pump light pulse at 525 nm. As shown in Figure 3e, photoexcitation of SC-Au/TiO<sub>2</sub> caused ground state bleaching at 550 nm, while no obvious signal for pristine TiO<sub>2</sub> and S-Au/TiO<sub>2</sub>,<sup>[35]</sup> confirming the role of Au nanoclusters as hot spots to concentrate incident light for generating hot charge carriers.<sup>[36]</sup> Meanwhile, retained Au single atoms with lower work function could serve as electron reservoirs to capture these hot electrons from TiO<sub>2</sub>, as evidenced by the positively shifted Fermi level of S-Au/TiO<sub>2</sub> (Figure S15). The further introduction of oxygen vacancies in TiO<sub>2</sub> induced larger interfacial band bending, proving new channels for shuttling energetic hot electrons from Au nanoclusters to adjacent TiO<sub>2</sub> supports, as reflected in the prolonged recovery lifetime of SC-Au/O<sub>v</sub>-TiO<sub>2</sub> in TAS analysis. Overall, the creation of multifarious sites generated a stronger built-in electric field to boost the charge separation (Figure S16), significantly increased the donor (electron) density (Table S3), and prolonged the carrier lifetimes (Figure 2f, Figure S17, and Table S4). Correspondingly, the cascade charge transfer in SC-Au/O<sub>v</sub>-TiO<sub>2</sub>, contributed to the 50-fold-increased visible light activity of reconstructed photocatalysts for plasmon resonance-enhanced photocatalysis (Figure S18).<sup>[37]</sup>

The hydrogen adsorption Gibbs free energies ( $\Delta G_H$ ) over sodium-stabilized Au single atoms were examined by theoretical calculations (Figure 4a). As shown in Figure 4b, the adsorption of one H onto isolated Au formed the structure of Au(1H) with a Gibbs free energy of -1.07 eV. The introduction of one Na<sup>+</sup> dramatically decreased  $\Delta G_H$ , with a minimum value of 0.03 eV for 1-Au(1H)(Na<sup>+</sup>). No further improvement was achieved with one more Na<sup>+</sup>, confirming the significant contribution of Au(Na<sup>+</sup>) interactions for HER activity. To investigate the downhill of  $\Delta G_H$ , the electronic structure of Au(1H)(Na<sup>+</sup>) was further explored by the density of states (DOS). From the projected density of states (PDOS) for Ti (Figure 4c), the emergence of Ti<sup>3+</sup> indicated the strong electronic coupling between Au, Na, and Ti. Compared to Au(1H) and 2-Au(1H)(Na<sup>+</sup>), the peak shape of Ti<sup>3+</sup> was much sharper in 1-Au(1H)(Na<sup>+</sup>) (Figure S19),

proving the capability of Au single atoms for electron reserving. Based on the PDOS for Au, Na, and H in Au(1H)(Na<sup>+</sup>), H-s orbital of Au(1H)(Na<sup>+</sup>) was occupied and located at a low energy level, which meant that it was easy to be desorbed from the Au site and thus promoted the hydrogen reduction ( $\text{H}^+ + \text{e}^- \rightarrow \text{H}_2$ ) (Figure 4d). Based on these results, we conclude that sodium not only played a critical role in the stabilization of isolated Au atoms for multi-site construction but also contributed to the reduced energy barrier for water splitting reaction.

**Versatility of photoreconstruction strategy.** The generality of our SPR strategy for developing efficient multi-site synergistic catalysts was demonstrated by various metal oxide and noble metals for versatile reactions. The introduction of Au single atoms (S-Au/BiOBr) enhanced the photoactivity of BiOBr for nitrogen fixation, while solid-state reconstruction (SC-Au/BiOBr) further doubled the ammonia production rate (Figure S20). Redispersal of Au single atoms was conducted to improve the performance of CeO<sub>2</sub> for CO oxidation (Figure S21). As shown in Figure 4e, the impregnation of CeO<sub>2</sub> nanorods by 0.5 wt% Au single atoms (S-Au/CeO<sub>2</sub>) decreased the complete conversion temperature from 350 °C to 80 °C. Photoreconstructed SC-Au/CeO<sub>2</sub> with synergistic sites could efficiently oxidize CO at room temperature, signifying its great potential for gas purification. We also performed solid-state reconstruction of Ru single atoms on TiO<sub>2</sub> for the enhanced catalytic conversion of biomass into aromatic compounds. As expected, the reconstructed SC-Ru/001-TiO<sub>2</sub> exhibited two and four times higher activity than S-Ru/001-TiO<sub>2</sub> with single site and benchmark Ru/P25, respectively (Figure 4f). The extended applications of our SPR strategy well demonstrated the significance of site engineering for the rational design of high-performance catalysts.

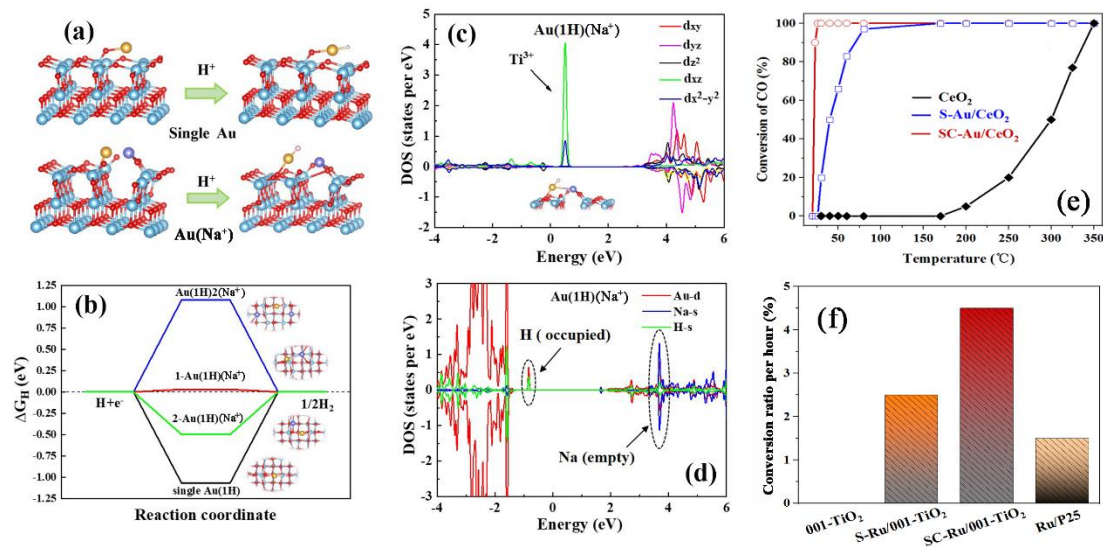


**Figure 4** (a) Local atomic structures of hydrogen adsorption configurations on single Au and Au-Na dimer. Blue, red, yellow, purple, and white spheres represented Ti, O, Au, Na, and H atoms, respectively. (b) The  $\Delta G_H$  for different Au sites mediated by Na<sup>+</sup>. Different sites were considered and the represented ones were denoted as 1-Au(1H)(Na<sup>+</sup>) and 2-Au(1H)(Na<sup>+</sup>). (c) The Projected DOS of Ti around Au-O bond in Au(1H)(Na<sup>+</sup>) dimer. (d) The Projected DOS of Au, Na, and H in Au(1H)(Na<sup>+</sup>). (e) Photoreconstruction of Au single atoms on CeO<sub>2</sub> significantly improved the room temperature activity for CO oxidation. (f) Photoreconstruction promoted the activity of Ru-cocatalyzed 001-TiO<sub>2</sub> for converting biomass into aromatic compounds. Phenyl ether was selected as a model of  $\alpha$ -O-4 and  $\beta$ -O-4 ether lignin intralinkages in woody biomass.

## Conclusions

In summary, we have successfully developed an SPR strategy to construct advanced catalysts with multifarious active sites for versatile applications. As demonstrated by experimental and theoretical investigations, Na<sup>+</sup> could stabilize noble metal single atoms through mediating the metal-support interactions, while light illumination of presynthesized powders induced the charge transfer from Ti<sup>3+</sup> to Au single atoms, facilitating their partial agglomeration into nanoclusters via solid-state reactions. The co-construction of Au nanoclusters and sodium-stabilized Au single atoms act as plasmonic hot spots and electron reservoirs, respectively. The further creation of

oxygen vacancies in TiO<sub>2</sub> promotes shuttling energetic hot electrons from Au nanoclusters to Au single crystals . The final reconstructed SC-Au/Ov-TiO<sub>2</sub> photocatalysts with the cascade charge transfer exhibited a nearly two orders of magnitude enhancement in hydrogen evolution than that of blank TiO<sub>2</sub> under simulated solar light. The TON<sub>Au</sub> reached a benchmark value of 4600 among all reported Au cocatalyzed TiO<sub>2</sub> photocatalysts. The SPR strategy could be easily extended to prepare a wide scope of noble metal cocatalyzed nanostructures with enhanced performance for kinds of catalytic reactions. This work not only provides new insights into comprehending and harnessing the metal-support interactions in SACs for activity enhancement but also opens a new avenue to construct advanced catalysts with multifarious sites for overcoming the current issues facing SACs.

### **Acknowledgment**

This work was supported by the National Natural Science Foundation of China (Grant no. 51978372, 52170042, 11974037). We would like to acknowledge the Beijing Synchrotron Radiation Facility (BSRF) for crystal diffraction data collection. This research was supported by the high performance computing (HPC) resources at Beihang University.

### **References**

- [1] Botao Qiao, Aiqin Wang, Xiaofeng Yang, Lawrence F. Allard, Zheng Jiang, Yitao Cui, Jingyue Liu, Jun Li, Tao Zhang, Single-atom catalysis of CO oxidation using Pt1/FeO<sub>x</sub>, *Nature Chemistry*, 2011, 3, 634.
- [2] Daobin Liu, Qun He, Shiqing Ding, Li Song, Structural Regulation and Support Coupling Effect of Single-Atom Catalysts for Heterogeneous Catalysis, *Adv. Energy mater*, 2020, 10, 2001482.
- [3] Jincheng Liu, Yan Tang, Yanggang Wang, Tao Zhang, Jun Li, Theoretical understanding of the stability of single-atom catalysts, *Natl. Sci. Rev.*, 2018, 5, 638.
- [4] Javier Pérez-Ramírez, Núria López, Strategies to break linear scaling relationships, *Nature Catalysis*, 2019, 2, 971.
- [5] Wenjie Zang, Zongkui Kou, Stephen J. Pennycook, John Wang, Heterogeneous

Single Atom Electrocatalysis, Where “Singles” Are “Married”, *Adv. Energy Mater.* 2020, 10, 5884.

[6] Xiaojuan Zhu, Qishui Guo, Yafei Sun, Shangjun Chen, Jian-Qiang Wang, Mengmeng Wu, Wenzhao Fu, Yanqiang Tang, Xuezhi Duan, De Chen, Ying Wan, Optimising surface d charge of AuPd nanoalloy catalysts for enhanced catalytic activity, *Nature Communication*, 2019, 10, 1428.

[7] Lei Zhang, Rutong Si, Hanshuo Liu, Ning Chen, Qi Wang, Keegan Adair, Zhiqiang Wang, Jiatang Chen, Zhongxin Song, Junjie Li, Mohammad Norouzi Banis, Ruying Li, Tsun-Kong Sham, Meng Gu, Li-Min Liu, Gianluigi A. Botton, Xueliang Sun, Atomic layer deposited Pt-Ru dual-metal dimers and identifying their active sites for hydrogen evolution reaction, *Nature Communication*, 2019, 10, 4936.

[8] Hongpan Rong, Shufang Ji, Jiatao Zhang, Dingsheng Wang, Yadong Li, Synthetic strategies of supported atomic clusters for heterogeneous catalysis, *Nature Communication*, 2020, 11, 5884.

[9] Xiaoqian Wei, Xin Luo, Nannan Wu, Wenling Gu, Yuehe Lin, Chengzhou Zhu, Recent advances in synergistically enhanced single-atomic site catalysts for boosted oxygen reduction reaction, *Nano Energy*, 2021, 84, 105817.

[10] Wei Xi, Kai Wang, Yongli Shen, Mengke Ge, Ziliang Deng, Yunfeng Zhao, Qiue Cao, Yi Ding, Guangzhi Hu, Jun Luo, Dynamic co-catalysis of Au single atoms and nanoporous Au for methane pyrolysis, *Nature Communication*, 2020, 11, 1919.

[11] Yifan Sun, Felipe Polo-Garzon, Zhenghong Bao, Jisue Moon, Zhennan Huang, Hao Chen, Zitao Chen, Zhenzhen Yang, Miaofang Chi, Zili Wu, Jue Liu, and Sheng Dai, Manipulating Copper Dispersion on Ceria for Enhanced Catalysis: A Nanocrystal-Based Atom-Trapping Strategy, *Adv. Sci.* 2022, 2104749.

[12] Wentao Yuan, Dawei Zhang, Yang Ou, Ke Fang, Beien Zhu, Hangsheng Yang, Thomas W. Hansen, Jakob B. Wagner, Ze Zhang, Yi Gao, Yong Wang, Direct In Situ TEM Visualization and Insight into the Facet-Dependent Sintering Behaviors of Gold on TiO<sub>2</sub>, *Angew. Chem. Int. Ed.* 2018, 57, 16827.

[13] Bing Han, Yalin Guo, Yike Huang, Wei Xi, Jie Xu, Jun Luo, Haifeng Qi, Yujing

- Ren, Xiaoyan Liu, Botao Qiao, Tao Zhang, Strong Metal–Support Interactions between Pt Single Atoms and TiO<sub>2</sub>, *Angew. Chem. Int. Ed.* 2020, 59, 11824–11829
- [14] Yanping Zhai, Danny Pierre, Rui Si, Weiling Deng, Peter Ferrin, Anand U. Nilekar, Guowen Peng, Jeffrey A. Herron, David C. Bell, Howard Saltsburg, Manos Mavrikakis, Maria Flytzani-Stephanopoulos, Alkali-Stabilized Pt-OH<sub>x</sub> Species Catalyze Low-Temperature Water-Gas Shift Reactions, *Science*, 2010, 329, 1633.
- [15] Jian Zhang, Hai Wang, Liang Wang, Sajjad Ali, Chengtao Wang, Lingxiang Wang, Xiangju Meng, Bo Li, Dang Sheng Su, Feng-Shou Xiao, Wet-Chemistry Strong Metal–Support Interactions in Titania-Supported Au Catalysts, *J. Am. Chem. Soc.* 2019, 141, 7, 2975–2983.
- [16] Rizwan Khan, Malenahalli H. Naveen, Muhammad A. Abbas, Junghyun Lee, Hahkjoon Kim, Jin Ho Bang, Photoelectrochemistry of Au Nanocluster-Sensitized TiO<sub>2</sub>: Intricacy Arising from the Light-Induced Transformation of Nanoclusters into Nanoparticles, *ACS Energy Lett.* 2021, 6, 24–32.
- [17] A. Naldoni, M. D’Arienzo, M. Altomare, M. Marelli, R. Scotti, F. Morazzoni, E. Selli, V. Dal Santo, *Appl. Catal. B-Environ.* 2013, 130-131, 239.
- [18] Y. Chang, Y. Xuan, H. Quan, H. Zhang, S. Liu, Z. Li, K. Yu, J. Cao, *Chem. Eng. J.* 2020, 382, 122869.
- [19] A. Chang, W.-S. Peng, I. T. Tsai, L.-F. Chiang, C.-M. Yang, *Appl. Catal. B-Environ.* 2019, 255, 117773.
- [20] C. K. Ngaw, Q. Xu, T. T. Y. Tan, P. Hu, S. Cao, J. S. C. Loo, *Chem. Eng. J.* 2014, 257, 112.
- [21] Z. H. N. Al-Azri, W.-T. Chen, A. Chan, V. Jovic, T. Ina, H. Idriss, G. I. N. Waterhouse, *J. Catal.* 2015, 329, 355.
- [22] Z. W. Seh, S. Liu, M. Low, S.-Y. Zhang, Z. Liu, A. Mlayah, M.-Y. Han, *Adv. Mater.* 2012, 24, 2310.
- [23] J. B. Priebe, J. Radnik, A. J. J. Lennox, M.-M. Pohl, M. Karnahl, D. Hollmann, K. Grabow, U. Bentrup, H. Junge, M. Beller, A. Brückner, *ACS Catal.* 2015, 5, 2137.
- [24] S. S. Rayalu, D. Jose, M. V. Joshi, P. A. Mangrulkar, K. Shrestha, K. Klabunde, *Appl. Catal. B-Environ.* 2013, 142-143, 684.



- [25] D. Ding, K. Liu, S. He, C. Gao, Y. Yin, *Nano Lett.* 2014, 14, 6731.
- [26] W.-T. Chen, A. Chan, Z. H. N. Al-Azri, A. G. Dosado, M. A. Nadeem, D. Sun-Waterhouse, H. Idriss, G. I. N. Waterhouse, *J. Catal.* 2015, 329, 499.
- [27] Junya Suetake, Atsuko Y. Nosaka, Kazunori Hodouchi, Hiroshi Matsubara, Yoshio Nosaka, Characteristics of Titanate Nanotube and the States of the Confined Sodium Ions, *J. Phys. Chem. C*, 2008, 112, 47, 18474.
- [28] Jun Li, Jian Liu, Qian Sun, Mohammad Norouzi Banis, Xueliang Sun, Tsun-Kong Sham, Tracking the Effect of Sodium Insertion/Extraction in Amorphous and Anatase TiO<sub>2</sub> Nanotubes, *J. Phys. Chem. C*, 2017, 121, 11773.
- [29] Mikaela Görlin, Joakim Halldin Stenlid, Sergey Koroidov, Hsin-Yi Wang, Mia Börner, Mikhail Shipilin, Aleksandr Kalinko, Vadim Murzin, Olga V. Safonova, Maarten Nachtegaal, Abdusalam Uheida, Joydeep Dutta, Matthias Bauer, Anders Nilsson, Oscar Diaz-Morales, Key activity descriptors of nickel-iron oxygen evolution electrocatalysts in the presence of alkali metal cations, *Nature Commun.* 2020, 11, 6181.
- [30] Ming Yang, Sha Li, Yuan Wang, Jeffrey A. Herron, Ye Xu, Lawrence F. Allard, Sungsik Lee, Jun Huang, Manos Mavrikakis, Maria Flytzani-Stephanopoulos, Catalytically active Au-O(OH)<sub>x</sub> species stabilized by alkali ions on zeolites and mesoporous oxides, *Science*, 2014, 346, 1498.
- [31] J. Wan, W. Chen, C. Jia, L. Zheng, J. Dong, X. Zheng, Y. Wang, W. Yan, C. Chen, Q. Peng, D. Wang, Y. Li, Defect Effects on TiO<sub>2</sub> Nanosheets: Stabilizing Single Atomic Site Au and Promoting Catalytic Properties, *Adv. Mater.* 2018, 30, 1705369.
- M. Yang, L. F. Allard, M. Flytzani-Stephanopoulos, Atomically Dispersed Au-(OH)<sub>x</sub> Species Bound on Titania Catalyze the Low-Temperature Water-Gas Shift Reaction, *J. Am. Chem. Soc.* 2013, 135, 3768–3771.
- [32] A. Michalowicz, J. J. Girerd, and J. Goulon, EXAFS [extended x-ray absorption fine structure] determination of the copper oxalate structure. Relation between structure and magnetic properties, *Inorg. Chem.* 1979, 18, 11, 3004–3010
- [33] H. Tang, Y. Su, B. Zhang, A. F. Lee, M. A. Isaacs, K. Wilson, L. Li, Y. Ren, J. Huang, M. Haruta, B. Qiao, X. Liu, C. Jin, D. Su, J. Wang, T. Zhang, *Sci. Adv.* 2017, 3, 1700231.

- [34] Y. Zhang, J. Liu, K. Qian, A. Jia, D. Li, L. Shi, J. Hu, J. Zhu, W. Huang, Structure Sensitivity of Au-TiO<sub>2</sub> Strong Metal–Support Interactions, *Angew. Chem. Int. Ed.* 2021, 60, 12074-12081.
- [35] Landong Li, Junqing Yan, Tuo Wang, Zhi-Jian Zhao, Jian Zhang, Jinlong Gong, Naijia Guan, Sub-10nm rutile titanium dioxide nanoparticles for efficient visible-light-driven photocatalytic hydrogen production, *Nature Commun.* 2015, 6, 5881.
- [36] Chengcheng Li, Tuo Wang, Zhi-Jian Zhao, Weimin Yang, Jian-Feng Li, Ang Li, Zhilin Yang, Geoffrey A. Ozin, Jinlong Gong, Promoted Fixation of Molecular Nitrogen with Surface Oxygen Vacancies on Plasmon-Enhanced TiO<sub>2</sub> Photoelectrodes, *Angew. Chem. Int. Ed.*, 2018, 57, 5278 –5282.
- [37] L. Collado, A. Reynal, F Fresno, M. Barawi, C. Escudero, V. Perez-Dieste, J. M. Coronado, D. P. Serrano, J R. Durrant, V A. de la Peña O’Shea, Unravelling the effect of charge dynamics at the plasmonic metal/semiconductor interface for CO<sub>2</sub> photoreduction, *Nature Communications*, 2018, 9, 4986.